MODELING AND OPTIMIZATION OF REFRIGERATION CASSETTES FOR LIGHT COMMERCIAL APPLICATIONS

Maicon Waltrich, maicon@polo.ufsc.br
Cláudio Melo, melo@polo.ufsc.br
Department of Mechanical Engineering, Federal University of Santa Catarina
88040970, Florianópolis-SC, Brazil, ++55 48 3721 9397

Christian J. L. Hermes, chermes@ufpr.br
Department of Mechanical Engineering, Federal University of Paraná
PO Box 19011, 81531990, Curitiba-PR, Brazil, ++55 41 3361 3239

Abstract. *A novel design methodology based on a model-driven optimization algorithm for sizing the components of refrigeration cassettes is presented herein. The approach was implemented and validated for a light commercial refrigeration system (i.e., a cooling capacity ranging from 0.5 to 1.5 kW), although it can be easily extended to any other vapor compression refrigeration unit. Mathematical models were obtained for each of the system components. A first-principles steady-state tri-dimensional model was developed to simulate the thermo-hydraulic performance of fan-supplied tube-fin heat exchangers (condenser and evaporator). Furthermore, a semi-empirical sub-model for the compressor was devised and combined with the heat exchanger sub-models in order to predict the thermodynamic performance of the entire refrigeration system. The numerical results were compared with experimental data taken with different cassettes in a specially constructed calorimeter testing facility. It was found that the model predictions for the working pressures, power consumption, cooling capacity and coefficient of performance (COP) were very close to the experimental data with maximum deviations of ±10%. In addition, a genetic optimization algorithm was used to design the condenser and evaporator and also to select the compressor model based on an objective function which considers both the COP and overall cost. The optimization led to two improved configurations, which were assembled and tested. One of the optimized systems showed a COP / cost ratio approximately two times higher than that of the original (baseline) cassette.*

Keywords*: commercial refrigeration, cassette, simulation, optimization, design.*

1. INTRODUCTION

Vapor compression refrigeration systems, on the whole, consume a large amount of energy since hundreds of millions are currently in use, and dozens of millions are coming onto the market every year. This fact has motivated governments worldwide are continually launching ever more stringent energy consumption policies for household and commercial refrigeration appliances. For instance, the labeling policy for light commercial refrigeration appliances will be deflagrated in 2011. In order to fulfill the new energy regulations most manufacturers are seeking alternative ways to improve the thermodynamic performance of their products.

Some of the beverage coolers currently on the market are composed of a thermally insulated cabinet and a compact cooling system, also known as a refrigeration cassette (see Fig. 1). In comparison to the conventional refrigeration systems, the cassette systems are easier to transport, to replace and to access for cleaning and maintenance.

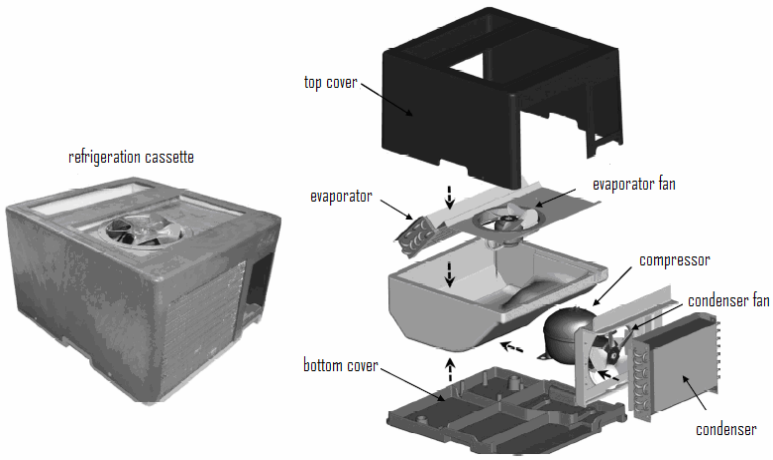

Figure 1. Schematic of the refrigeration cassette

The cassette refrigeration system comprises two fan-supplied tube-fin heat exchangers (evaporator and condenser), a reciprocating hermetic compressor, and a thermostatic expansion valve. Additional components such as a pre-condenser and a liquid-line/suction-line heat exchanger (also known as internal heat exchanger) are also employed. The air streams through the condenser and the evaporator are separated from each other by polyurethane insulation. Of these components, the compressor and the heat exchangers are those which have a major impact both on the system coefficient of performance (*COP*) and the cost. The compressor selection and the heat exchanger design usually follow standardized test procedures (e.g., SE-SP-200 to 204, 2006), which are costly and time consuming. Alternatively, mathematical models can be employed to reduce the amount of prototypes and experimental runs required. Several publications can be found in the literature with an emphasis on the numerical simulation of refrigeration systems (Hermes and Melo, 2008; Gonçalves et al., 2009; Hermes et al., 2009; Borges et al., 2010), but optimization studies for component sizing are scarce. Furthermore, the reported studies treat one component at a time (Bansal and Chin, 2003; Stewart *et al*., 2005; Gholap and Khan, 2007), neglecting the intrinsic relationship between the system components. In this context, a numerical simulation model for the entire refrigeration system was developed, validated and employed to optimize the cassette design by simultaneously varying the compressor, condenser and the evaporator features.

2. SIMULATION MODEL

The mathematical formulation employed follows that originally proposed by Hermes et al. (2009) for household refrigerators. The system simulation model was divided into the following sub-models (see Fig. 2): compressor, pre-condenser, air-supplied heat exchangers (condenser and evaporator), and liquid-line/suction-line heat exchanger.

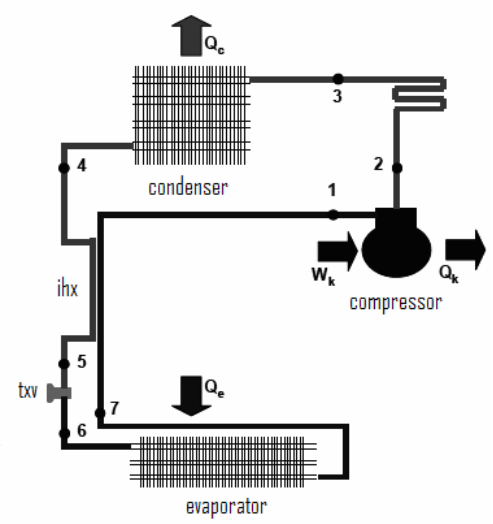

Figure 2. Schematic of the refrigeration loop

2.1 Fan-supplied tube-fin heat exchangers (condenser and evaporator)

The heat exchangers were modeled according to the approach proposed by Waltrich et al. (2010), which consists of adopting two sub-models, one for heat transfer and another for pressure drop (see Fig. 3). The thermal sub-model was divided into two domains, namely the air and refrigerant sides. The thermal resistances to conduction through the tube and fin walls were neglected. Both the air and refrigerant flows were modeled as one-dimensional, steady-state and purely advective flows. The heat transfer rate Qcv was calculated from the concept of heat exchanger effectiveness, as follows:

$$Q_{cv} = \pm\varepsilon_{cv} C_{min}\left(t_{i,h} - t_{i,c}\right) = m_r \Delta h_r \tag{1}$$

where the "–" sign applies to condensers and gas coolers and the "+" sign to evaporators, $C_{min}=min(m_r c_{p,r}, m_{a,cv} c_{p,a})$ is the lowest thermal capacity [W/K] of the streams, and $t_{i,h}$ and $t_{i,c}$ are the temperatures of the hot and cold streams at the entrance ports [K], respectively.

The control volume effectiveness ε for a mixed, cross-flow, single-pass heat exchanger was calculated as follows (Kays and London, 1999):

$$\varepsilon_{cv} = 1 - \exp\left(NTU^{0.22} C_r^{-1}\left(\exp\left(-C_r NTU^{0.78}\right) - 1\right)\right) \tag{2}$$

where $C_r=C_{min}/C_{max}$, and $NTU=UA/C_{min}$ is the number of transfer units. The fin efficiency was calculated by the procedure introduced by Schmidt (1945), and the heat transfer coefficients were obtained from empirical correlations. The air-side heat transfer coefficients were calculated from the correlation proposed by Wang *et al.* (2000), and the heat transfer coefficients for the refrigerant side were derived from Gnielisnki's (1976) correlation for single-phase flows, and assumed to be infinite for condensing and evaporating flows of HFC-134a.

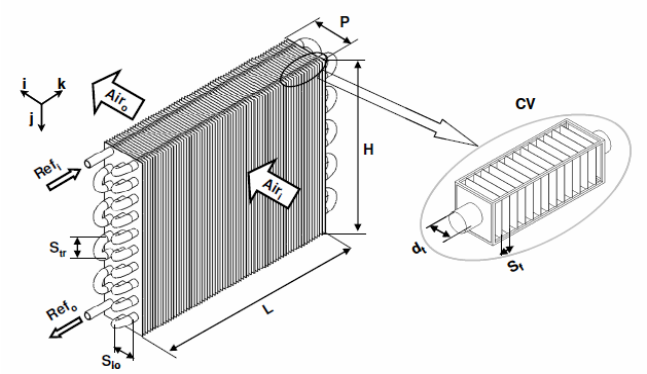

Figure 3. Physical model of the heat exchangers

The hydrodynamic sub-model considers the heat exchanger pressure drop and also the fan-supplied air flow rate. The air flow rate is dependent on both (i) the fan characteristics and ii) the system impedance created by the evaporator, supply and return ducts, refrigerated compartment and fan hood, arranged in a closed loop for the cold air stream and by the condenser, fan hood and grills, arranged in an open-loop for the warm air stream. Therefore, the evaporator fan pressure head is calculated from $\Delta p_e=\Delta p_{1\text{-}2}=\Delta p_{2\text{-}3}+\Delta p_{3\text{-}1}$, where the term $\Delta p_{2\text{-}3}$ corresponds to the pressure drop in the evaporator coil, and $\Delta p_{3\text{-}1}$ is the pressure loss in the refrigerated compartment (see Fig. 4). The condenser fan pressure head is calculated from $\Delta p_c=\Delta p_{6\text{-}7}=\Delta p_{5\text{-}6}+\Delta p_{7\text{-}8}$, where the term $\Delta p_{5\text{-}6}$ corresponds to the pressure drop in the condenser coil, and $\Delta p_{7\text{-}8}$ is the pressure drop at the outlet port (see Fig. 4). The performance characteristics of the evaporator and condenser fans were expressed as sixth-order polynomials.

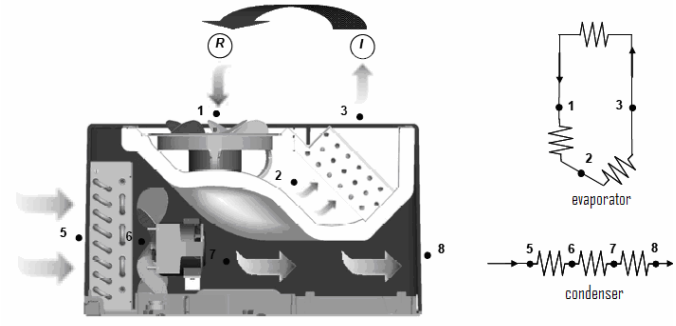

Figure 4. Schematic of the air circuit

The solution algorithm employs two loops. Firstly, the hydrodynamic sub-model is iteratively solved to obtain the fan-supplied air flow rate. Secondly, the thermal sub-model is also iteratively solved for each control volume through a one-way march following the refrigerant circuit. The procedure is repeated until convergence is achieved, i.e., when the largest temperature difference between two successive iterations is less than 0.1°C. Comparisons with experimental results showed that the model was able to predict 92% of the experimental data for the heat transfer rate with a maximum deviation of ±10%, and 88% of the experimental data for the pressure drop with a maximum deviation of ±15%. More details can be found in Waltrich *et al.* (2010).

2.2 Compressor, pre-condenser and internal heat exchanger

In most reciprocating compressors the refrigerant passes successively through the compressor shell, the suction muffler and the suction valve before entering the compression chamber from where it is pumped through the discharge valve and then through the discharge muffler to the condenser. The refrigerant enthalpy at the compressor discharge, h_2, is calculated from an energy balance at the compressor shell,

$$h_2 = h_1 + \left(W_k - Q_k\right)/m_r \tag{3}$$

The compressor mass flow rate, m_r, and the compression power, W_k, are, respectively, obtained from

$$m_r = \eta_v V_k N / v_1 \tag{4}$$

$$W_k = m_r (h_{2,s} - h_1) / \eta_g \tag{5}$$

The rate of heat released from the compressor shell, Q_k, is calculated from

$$Q_k = U_k A_{shell} (t_2 - t_a) \tag{6}$$

The volumetric and overall efficiencies, η_v and η_g, and the overall thermal conductance (U_k) of the compressor were all obtained from experimental tests carried out with the cassette. The volumetric and overall efficiencies were fitted as linear functions of the pressure ratio, p_c/p_e, while the thermal conductance, U_k, was assumed to be constant (= 14 W/m^{2}K). The shell surface area, A_{shell}, was supplied by the compressor manufacturer.

The pre-condenser is a gas cooler placed between the compressor and the condenser, and thus an equation is required to calculate the refrigerant enthalpy at the condenser inlet:

$$h_3 = h_2 + c_{p,r}(t_2 - t_a)\left[1 - exp\left(-U_{pc} A_{pc} / m_r c_{p,r}\right)\right] \tag{7}$$

where the heat transfer coefficient at the refrigerant side was calculated from the Gnielinski (1976) correlation, and the air side heat transfer coefficient was assumed to be constant (= 38 W/m^{2}K).
The cassette employs a lateral liquid-line/suction-line heat exchanger. The refrigerant enthalpy at the entrance of the expansion device (see Fig. 2), h_6, was obtained from the following energy balance:

$$h_6 = h_5 = h_4 + h_7 - h_1 \tag{8}$$

where $t_1 = t_7 + \varepsilon_{ihx}(t_4 - t_5)$, and ε_{ihx} was obtained experimentally.

2.3 Working pressures

Two additional equations are required to determine the evaporating and condensing pressures. In general, the working pressures are obtained implicitly and iteratively considering that the mass flow rate through the expansion device is equal to that discharged by the compressor, and also that the amount of refrigerant inside the refrigeration loop is fixed. However, it is worth noting that such a formulation is a strongly non-linear implicit function of the working pressures, leading to time-consuming calculations and also to convergence issues. In order to keep a reasonable level of complexity, it has been assumed that the refrigerant superheating and subcooling at the evaporator and condenser exits are fixed (see Hermes et al., 2009).

2.4 Solution methodology

The code was implemented using the EES platform (Klein and Alvarado, 2004) and the REFPROP7 software program (Lemmon *et al*., 2002). The solution algorithm follows the procedure introduced by Hermes *et al.* (2009), where two iterative loops are adopted. The input parameters are the air temperature at the condenser and evaporator inlets, the evaporator superheating and condenser subcooling, the compressor speed, and all the empirical parameters obtained from the experiments. In the outer loop, the condensing and evaporating pressures and the refrigerant temperature at the compressor inlet are calculated by the Newton-Raphson method. In the inner loop, a successive substitution scheme was adopted for each of the system components. Thus, for a given set of values for p_e, p_c and t_1, the compressor sub-model calculates h_2, the condenser sub-model estimates h_4 and $t_4 = t(p_c, h_4)$, the internal heat exchanger sub-model calculates h_6 and t_1, and the evaporator sub-model calculates h_7 and $t_7 = t(p_e, h_7)$. The calculation procedure continues until convergence is achieved.

3. OPTIMIZATION SCHEME

The optimization of a refrigeration system is very much dependent on the choice of an objective function (also known as performance evaluation criterion, *PEC*). In this study, the following *PEC* was devised in order to consider both the thermodynamic (*COP*) and economic (cost, $) performances:

$$PEC = \left(COP/\$_{tot}\right)_{optimized} / \left(COP/\$_{tot}\right)_{baseline} \tag{9}$$

where $\$_{tot}$ is the total cost, which considers the cost of each system component based on the following assumptions:

- **Cost data:** The cost analysis was based on real cost data so that the real trends are properly reproduced by the model. However, a fictitious monetary unit (FMU) was employed as the cost information is classified.
- **Compressor:** The compressor cost was estimated from $\$_k=F_\$(COP\cdot Q_e)^{1/2}$, where both $1.5 < COP < 2.75$ W/W and $460 < Q_e < 750$ W were obtained from catalog data for evaporating and condenser temperatures of -10°C and 45°C, respectively. A fictitious monetary correction factor $F_\$=0.68$ FMU/W$^{1/2}$ was applied based on the real cost of the compressors.
- **Heat Exchangers:** The costs of the heat exchangers were obtained based on the amount of raw material employed (80%) and on the cost of manufacturing (20%), thus: $\$_{hx}=1.25(M_{Cu}\$_{Cu}+M_{Al}\$_{Al})$, where $\$_{Cu}=4.5\cdot\$_{Al}$, in [FMU/kg], and M_{Cu} and M_{Al} are given in [kg].
- **Fans and Accessories:** The cost of the fans were kept constant (7.20 FMU each), and the costs of the other accessories were considered to be 44.30 FMU.

The optimization analysis was conducted taking into account the constructive characteristics of the evaporator and the condenser, and also considering five different compressors (see Table 1). The restrictions were imposed by the test standards for "small" refrigeration cassettes (SE-SP-200 to 204, 2006): under condition "C", the system *COP* shall not be less than 1.0, whilst the cooling capacity shall not be less than 230 W under condition "D-2". The optimization was carried out using the genetic algorithm procedure available in EES.

Table 1. Heat exchanger and compressor characteristics

Evaporator			Condenser			Compressor			
Parameter	Min	Max	Parameter	Min	Max	Model	V_k [cm^3]	Q_e [W]	*COP*
Width, m	0.3	0.38	Width, m	0.2	0.304	Comp 1	16.8	747	1.49
Height, m	0.076	0.175	Height, m	0.152	0.275	Comp 2	10.61	643	2.21
Depth, m	0.044	0.088	Depth, m	0.044	0.088	Comp 3	7.95	599	2.15
Fin pitch, m	0.002	0.008	Fin pitch, m	0.001	0.006	Comp 4	7.95	620	2.74
Tube O.D., m	0.0075	0.0115	Tube O.D., m	0.0075	0.0115	Comp 5	7.69	457	1.92

4. EXPERIMENTAL WORK

4.1 Experimental facility

The experimental activities were carried out using a calorimeter purpose-built to test refrigeration cassettes, as shown in Fig. 5. The air supplied by the evaporator fan (R) is cooled down by the evaporator coil and then directed toward a polyurethane-insulated chamber, where a booster fan sets the pressure drop inside the chamber, whilst PID-controlled electrical heaters regulate the air temperature. A plenum is also employed to homogenize both the chamber air velocity and temperature. The cassette is properly attached to the cabinet in order to avoid any air and moisture infiltration. T-type thermocouples are placed within the chamber to provide the temperature distribution along the air circuit. A differential pressure transducer is also used to measure the pressure drop between the chamber inlet (I) and outlet (R) ports. The operation limits of the calorimeter are: maximum cassette size of 530 mm x 330 mm; maximum cabinet pressure drop of 125 Pa; and maximum heating power of 1874 W.

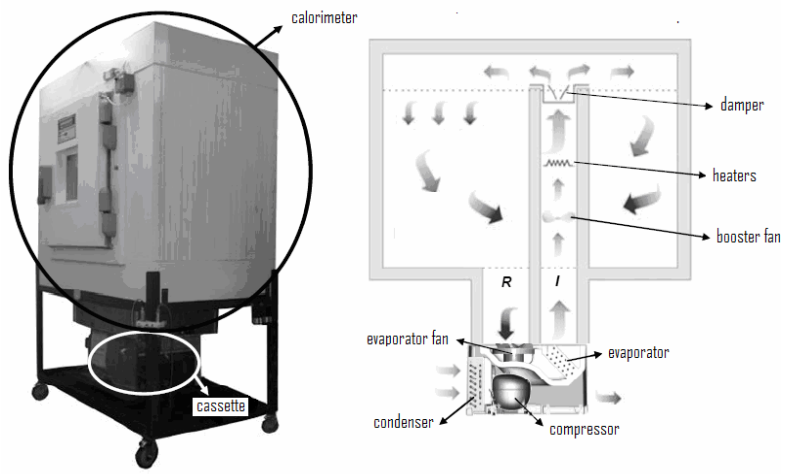

Figure 5. Schematic representation of the calorimeter

The cassette is instrumented with pressure transducers and T-type thermocouples according to the recommendations of the SE-SP-200 to 204 standards (2006), and the compressor power input is measured by a Yokogawa WT-230 power meter. The condenser and evaporator fan power inputs are measured beforehand. A computer-based data acquisition system is used to gather and process the experimental information. The calorimeter is placed inside an environmental room, with controlled indoor air temperature, humidity and velocity. The test conditions are then adjusted, and the cassette is kept on for 4 hours until the steady-state regime is achieved.

4.2 Test conditions

The test conditions are defined by the SE-SP-200 to 204 standards (2006), which set the approval criteria depending on the cassette size and weight. Two sets of ambient temperature and humidity are considered: 32.2ºC / 65% under condition "C" and 40.5ºC / 75% under conditions "D-2", "D-20" and "D-38". The air return temperature is 2 ºC under conditions "C" and "D-2", 20ºC under condition "D-20", and 38ºC under condition "D-38". For "small" cassettes, i.e. 0.324 m (height), 0.508 m (width), 0.559 m (depth) and 22 kg (weight), the minimum evaporator air flow rate and pressure drop relationships are 255 m^3/h (0 Pa), 212 m^3/h (25 Pa) and 190 m^3/h (37 Pa). Moreover, three other go/no go criteria are: (i) COP>1 under "C" condition; (ii) Q_e>230 W under "D-2" condition; (iii) ($Q_{e,\text{D-2}}$+$Q_{e,\text{D-20}}$+$Q_{e,\text{D-38}}$)>1500 W. Therefore, the product approval requires that at least five experimental tests are conducted. In this study, four different "small" refrigeration cassettes running with HFC-134a were tested according to the recommendations of the SE-SP-200 to 204 standards (2006) using various expansion valve and refrigerant charge adjustments, and also different compressors and heat exchanger configurations. In total, 59 experimental data points were collected. The geometric characteristics of the components tested (evaporators, condensers, fans and compressors) are shown in Tab. 3.

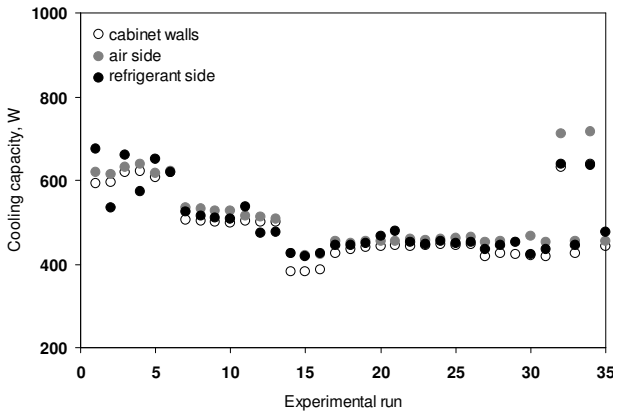

Figure 6. Comparison of the calculation procedures

Table 3. Construction characteristics of the cassettes

	Cassette	C1	C2	O1	O2
	Compressor	NEK6214Z	EMT6170Z	EGZS100 HLC	EGZS100 HLC
Condenser	Width	0.304	0.304	0.304	0.210
	Height / No. of transversal tubes	0.250 / 10	0.200 / 8	0.275 / 11	0.200 / 8
	Depth / No. of longitudinal tubes	0.066 / 3	0.066 / 3	0.088 / 4	0.044 / 2
	Fin pitch / No. of fins	0.0031 / 99	0.0034 / 90	0.0025 / 120	0.00175 / 120
	Tube O.D.	0.0095	0.0095	0.0075	0.0075
Evaporator	Width	0.380	0.380	0.380	0.300
	Height / No. of transversal tubes	0.200 / 8	0.150 / 6	0.175 / 7	0.150 / 6
	Depth / No. of longitudinal tubes	0.066 / 3	0.066 / 3	0.088 / 4	0.044 / 2
	Fin pitch / No. of fins	0.0035 / 108	0.0042 / 90	0.0025 / 150	0.0020 / 150
	Tube O.D.	0.0080	0.0080	0.0095	0.0095

4.3 Data processing

The cassette input power corresponds to the sum of the compressor power, W_k, with the power of the heat exchanger fans, W_e and W_c. The cassette cooling capacity was calculated using the three different approaches described below. The first approach considers an overall energy balance involving both the chamber and the cassette,

$$Q_e = UA_w\left(t_a - t_i\right) + k_r A_r \left(t_a + t_d - t_r - t_i\right)/2l_r + W_h + W_b + W_e \quad , \quad UA_w = 4.20 - 0.00978 \cdot \left(t_a - t_i\right) \tag{10}$$

The other approaches consider an energy balance on the refrigerant and air sides, respectively,

$$Q_e = m_r(h_7 - h_6) = m_r(h_1 - h_4) \tag{11}$$

$$Q_e = m_a c_{p,a}(t_r - t_i) + W_e \tag{12}$$

It is worthy of note that the refrigerant side cooling capacity was calculated from the refrigerant enthalpies at points (1) and (4), where there are only single-phase flows. Figure 6 compares the calculated cooling capacities derived from the three methodologies for all 59 experiments. It is shown that for most of the data runs the results are quite similar, with a maximum deviation of 10%.

5. RESULTS

5.1 Model validation

The experimental data used for the model validation exercise were obtained from the refrigeration cassettes C1 and C2 assembled with different compressors and heat exchangers, but with all other components remaining unchanged (e.g., fans, thermostatic expansion valve and internal heat exchanger). In total, 59 experimental runs were carried out under the "C" and "D" conditions of standards SE-SP-200 to 204 (2006), and with the condenser subcooling varying from 1 to 11°C and the evaporator superheating from 1 to 18°C. Figure 7 compares the measured working pressures (left), cooling capacities and power consumptions (right) with their simulated counterparts. It is shown that the model predictions are close to the experimental data with a maximum deviation of ±10%.

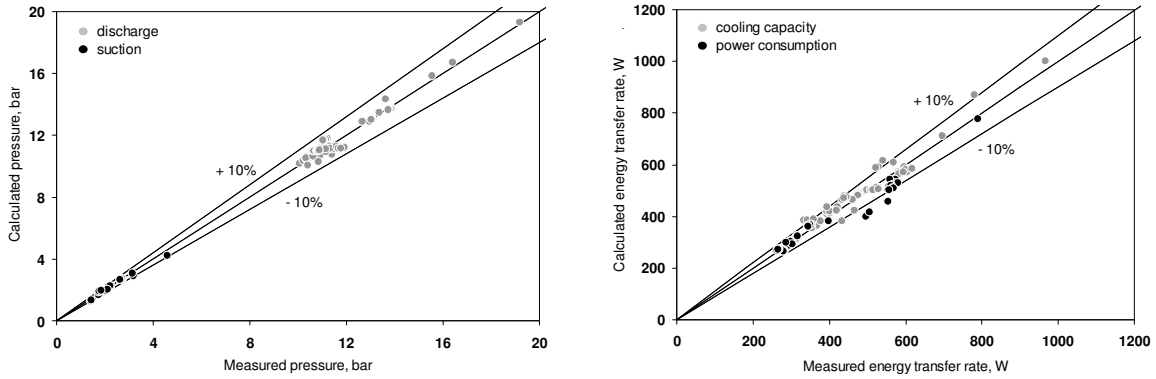

Figure 7. Comparison between calculated and measured working pressures (left) and energy transfer rates (right)

5.2 Cassette optimization

Cassette C2 was chosen as the baseline for the optimization processes since it provided the highest *COP*/cost ratio. The optimizations were performed under condition "C" assuming that both the evaporator superheating and the condenser subcooling are equal to 3°C. Two optimization criteria were adopted: (i) maximum *COP*, and (ii) maximum *PEC*=*COP*/$_{tot}$, giving rise to two different cassette configurations, namely O1 (*COP*-based) and O2 (*PEC*-based). The optimized cassette characteristics are presented in Table 3. Each optimization process required almost 3 hours to be completed. The results are summarized in Table 4. It is worth noting that the *COP* of cassette O1 is 53% higher than that of the baseline with additional evaporator and condenser costs of 31% and 42%, respectively, and with a compressor cost reduction of 18%. Although the heat exchangers became more expensive, the final cost of cassette O1 is lower than that of the baseline (see Table 4). Cassette O2, on the other hand, showed a COP 27% higher than that of the baseline, with cost reductions of 44%, 48% and 18% for the evaporator, condenser and compressor, respectively.

Table 4. Comparison between simulated and calculated results

Variable	C2			O1			O2		
	Exp.	Sim.	Diff.	Exp.	Sim.	Diff.	Exp.	Sim.	Diff.
p_e, bar	2.2	2.3	-0.1	2.1	2.1	0	1.8	1.9	-0.1
p_c, bar	10.3	10.6	-0.3	10.4	10.5	-0.1	10.9	11.7	-0.8
W_{tot}, W	299.4	303.1	-1.2%	279.5	266.1	4.8%	264.7	270	-2.0%
Q_e, W	419.5	423.6	-1.0%	561.2	567.5	-1.1%	439	469.4	-6.9%
COP	1.40	1.40	0.0%	2.01	2.13	-6.0%	1.66	1.74	-4.8%
Cost, FMU	88.15			86.50			81.50		

Cassettes O1 and O2 were manufactured and tested in order to validate the optimization methodology. The expansion device opening and the refrigerant charge of these cassettes were previously adjusted. Cassettes O1 and O2 were tested with a refrigerant charge of 500g and 200g, respectively, values that are quite different from that of cassette C2 (260 g) The difference between the refrigerant charges of cassettes O1 and O2 is mostly due to the different internal volumes of the heat exchanger coils. Table 4 compares the experimental (condition "C") and calculated results for cassettes C2, O1 and O2. It can be observed that the simulation results are in good agreement with the experimental counterparts, with differences of around ±5% for all the relevant parameters (*COP*, cooling capacity, working pressures, power consumption). Finally, it should be noted that the optimized cassettes surpassed the standardized requirements, with higher cooling capacities (65% (O1) and 39% (O2)) and higher COPs (105% (O1) and 65% (O2)). Another point to be noted is that during the tests under condition "D-38" the compressor thermal fuse, originally of 2.4A, was replaced by another of 2.7A, in order to keep the compressor running.

6. CONCLUDING REMARKS

A computer-aided engineering methodology for the design, analysis and optimization of refrigeration cassettes for light commercial applications was introduced herein. Mathematical models were proposed for each of the system components; particularly the fan-supplied tube-fin heat exchangers (condenser and evaporator) as they affect significantly both the system performance and product cost. Furthermore, the component sub-models were applied together in order to simulate the thermal behavior of the refrigeration cassette. It was found that the model predictions for the working pressures, power consumption, cooling capacity and *COP* are very close to the experimental data with maximum deviations of ±10%. The system simulation model was invoked by a genetic optimization algorithm that searches for *COP* and cost improvements by simultaneously changing the heat exchanger design characteristics and the compressor model. The optimization exercise provided two improved cassette configurations, which were assembled and tested in a purpose-built calorimeter apparatus. The optimized cassette configuration showed a *COP* / cost ratio almost two times higher than that of the baseline cassette.

7. ACKNOWLEDGEMENTS

This study was carried out at the POLO facilities under National Grant No. 573581/2008-8 (National Institute of Science and Technology in Refrigeration and Thermophysics) funded by the CNPq Agency. Financial and technical support from Embraco S.A. is also duly acknowledged. The authors also gratefully thank Messrs. Paulo C. Sedrez and Silvano Nunes for their valuable support with the experiments.

8. REFERENCES

ANEEL, Brazilian Atlas of Electrical Energy, National Agency of Electrical Energy, Brasília-DF, Brazil

Bansal PK, Chin TC, Modelling and optimization of wire-and-tube condenser, Int. J. Refrig., 26 (2003) 601-613

Borges BN, Hermes CJL, Goncalves JM, Melo C, 2010, Transient Simulation of Household Refrigerators: A Semi-Empirical, Quasi-Steady Approach, Int. Refrig. Conf. at Purdue, West Lafayette, USA, Paper 2122

Gholap AK, Khan JA, Design and multi-objective optimization of heat exchangers for refrigerators, Applied Energy, 84 (2007) 1226-1239

Gnielinski V, New equations for heat and mass transfer in turbulent pipe and channel flow, Int. Chem. Eng., 16 (1976) 359-368

Gonçalves JM, Melo C, Hermes CJL, A semi-empirical model for steady-state simulation of household refrigerators, A semi-empirical model for steady-state simulation of household refrigerators, Applied Thermal Engineering, Volume 29, Issues 8-9, June 2009, Pages 1622-1630

Hermes CJL, Melo C, A first-principles simulation model for the start-up and cycling transients of household refrigerators, International Journal of Refrigeration, Volume 31, Issue 8, December 2008, Pages 1341-1357

Hermes CJL, Melo C, Knabben FT, Gonçalves JM, Prediction of the energy consumption of household refrigerators and freezers via steady-state simulation, Applied Energy, 86 (2009) 1311-1319

Kays WM, London AL, Compact Heat Exchanger, Krieger Publishing, Boca Raton-FL, USA, 1999

Klein SA, Alvarado FL, Engineering Equation Solver User's Manual, F-Chart Software, Middleton-WI, USA, 2004

Lemmon EW, McLinden MO, Huber M.L., NIST Reference fluids thermodynamic and transport properties – REFPROP 7.0, Standard Reference Database 23, NIST, Gaithersburg, MD, USA, 2002

Marcinichen JB, Melo C, Reis EE, Schurt L, Experimental evaluation of the performance of refrigeration cassettes, II Iberian-American Congress of Cooling Science and Technology, Porto, Portugal, 2007 (in Portuguese)

Schmidt TE, La Production Calorifique dês Surfaces Munies D'ailettes, Bulletin de L'Institut International du Froid, Annexe G-5, 1945

SE-SP-200 to 204, Refrigeration cassette test standards, The Coca-Cola Company, Atlanta-GA, USA, 2006

Stewart SW, Shelton SS, Aspelund KA, Finned-tube Heat Exchanger optimization Methodology, Heat Transfer Engineering, 26 (2005) 22-28

Waltrich M, Hermes CJL, Goncalves JM, Melo C, A first-principles simulation model for the thermo-hydraulic performance of fan supplied tube-fin heat exchangers, Applied Thermal Engineering 30 (2010) 2011-2018

Wang CC, Chi KY, Chang CJ, Heat transfer and friction characteristics of plain fin-and-tube exchangers, Part II: Correlation, Int. J. Heat Mass Transfer, 43 (2000) 2693-2700

9. NOMENCLATURE

Roman

$\$$	Cost	[FMU]
A	Area	[m^2]
C	Thermal capacity	[W/K]
COP	Coefficient of performance	
c_p	Specific heat at constant pressure	[J/kgK]
d	Tube I.D.	[m]
e	Thickness	[m]
G	Mass flux	[kg/m^2s]
h	Enthalpy	[J/kg]
H	Heat exchanger height	[m]
k	Thermal conductivity	[K/W]
L	Heat exchanger width	[m]
m	Mass flow rate	[kg/s]
M	Mass	[kg]
N	Compressor speed	[rps]
N_t	Number of tube rows	
NTU	Number of transfer units	
p	Pressure	[Pa]
PEC	Performance evaluation criterion	
Q	Heat transfer rate	[W]
t	Temperature	[K]
UA	Thermal conductance	[W/K]
W	Power	[W]

Greek

α	Heat transfer coefficient	[W/m^2K]
ε	Heat exchanger effectiveness	
η	Efficiency	

Subscripts

1-7	positions along the refrigeration loop
a	ambient, air
b	booster fan
cv	control volume
d	discharge
e	evaporator
g	overall
h	heaters
i	inlet
ihx	internal heat exchanger
k	compressor
l	liquid
pc	pre-condenser
r	refrigerant, return
s	isentropic process
sat	saturated
sub	subcooled
sup	superheated
v	volumetric, vapor
w	calorimeter walls
x	expansion device